

Non-perturbative determination of c_V , Z_V and Z_S/Z_P in $N_f = 3$ lattice QCD*

Jochen Heitger^{1, **}, Fabian Joswig¹, Anastassios Vladikas², and Christian Wittemeier¹

¹Westfälische Wilhelms-Universität Münster, Institut für Theoretische Physik, Wilhelm-Klemm-Straße 9, 48149 Münster, Germany

²INFN, Sezione di Tor Vergata, c/o Dipartimento di Fisica, Università di Roma Tor Vergata, Via della Ricerca Scientifica 1, 00133 Rome, Italy

Abstract. We report on non-perturbative computations of the improvement coefficient c_V and the renormalization factor Z_V of the vector current in three-flavour $O(a)$ improved lattice QCD with Wilson quarks and tree-level Symanzik improved gauge action. To reduce finite quark mass effects, our improvement and normalization conditions exploit massive chiral Ward identities formulated in the Schrödinger functional setup, which also allow deriving a new method to extract the ratio Z_S/Z_P of scalar to pseudoscalar renormalization constants. We present preliminary results of a numerical evaluation of Z_V and c_V along a line of constant physics with gauge couplings corresponding to lattice spacings of about 0.09 fm and below, relevant for phenomenological applications.

1 Introduction

A popular discretization for quark fields on the lattice are Wilson fermions. However, as a consequence of removing the unwanted doublers in the naive lattice fermion action, it exhibits leading cutoff effects of $O(a)$ and the explicit breaking of chiral symmetry. As for the former, a systematic way of resolving this is the Symanzik improvement programme, which amounts to add the so-called clover term to the action and further irrelevant operators to local composite fields, canceling their $O(a)$ corrections, while the latter is accounted for by introducing finite renormalization constants. To eliminate all $O(a)$ contributions from physical quantities and to restore chiral symmetry at this order, these improvement counterterms and renormalization factors have to be fixed non-perturbatively.

In this work we specifically look at the renormalized and improved isovector current, which in the chiral limit of vanishing sea quark masses and at non-zero valence quark mass can be parametrized as

$$(V_R)_\mu^a(x) = Z_V(1 + b_V am_q)(V_I)_\mu^a(x), \quad (1)$$

with

$$(V_I)_\mu^a(x) = V_\mu^a(x) + ac_V \tilde{\partial}_V T_{\mu\nu}^a(x) \quad (2)$$

$$= \bar{\psi}(x) \gamma_\mu \frac{\tau^a}{2} \psi(x) + iac_V \tilde{\partial}_V \bar{\psi}(x) \sigma_{\mu\nu} \frac{\tau^a}{2} \psi(x), \quad (3)$$

*Talk at the 35th International Symposium on Lattice Field Theory (LATTICE 2017), 18-24 June 2017, Granada, Spain

**Speaker, e-mail: heitger@uni-muenster.de

where τ^a acts in flavour space and $\tilde{\partial}_\mu$ denotes the symmetric lattice derivative. The quark mass dependent $O(a)$ improvement term proportional to b_V , which corrects for quark mass dependent cutoff effects, was recently calculated non-perturbatively for $N_f = 3$ in [1, 2]. The renormalization constant Z_V and the improvement factor c_V , however, have not yet been investigated non-perturbatively so far in the case of three-flavour QCD and are subject to this work. Potential applications of the vector current and its matrix elements include computations of semi-leptonic decay form factors and of the timelike pion form factor, as well as contributions to the anomalous magnetic moment of the muon and thermal correlators related to the di-lepton production rate in the quark-gluon plasma.

Another object of interest is the ratio Z_S/Z_P of the scalar and the pseudoscalar renormalization constants, which plays a rôle in relating renormalized PCAC and subtracted quark masses to each other. The two constants themselves exhibit a scale dependence that cancels in the ratio, though. Accordingly, in the zero sea quark mass limit and at non-vanishing valence quark mass, the corresponding renormalized currents are defined as

$$(S_R)^a(x) = Z_S(1 + b_S am_q)\bar{\psi}(x)\frac{\tau^a}{2}\psi(x), \quad (P_R)^a(x) = Z_P(1 + b_P am_q)\bar{\psi}(x)\gamma_5\frac{\tau^a}{2}\psi(x) \quad (4)$$

and already comply with $O(a)$ improvement without any correction terms.

2 Renormalization and improvement conditions

All improvement and renormalization conditions explained below involve the $O(a)$ improved PCAC quark mass defined as

$$m_{\text{PCAC}} = \frac{\tilde{\partial}_0 f_A(x) + ac_A \partial_0^* \partial_0 f_P(x)}{2f_P(x)}, \quad (5)$$

with standard notation for (symmetric, backward and forward) lattice derivatives and where c_A for $O(a)$ improved $N_f = 3$ lattice QCD with Wilson fermions [3] and tree-level improved gauge action, as employed here, is non-perturbatively known from [4].

Let us mention that there exists a very promising alternative approach to determine renormalization factors through imposing appropriate conditions based on the PCAC relation in the Schrödinger functional with chirally rotated boundary conditions, see [5], where it was also tested in perturbation theory. Apart from its advantage of entailing automatic $O(a)$ improvement, it turned out that, e.g., in case of the renormalization factor of the axial current for $N_f = 2$, more precise results than with standard Schrödinger functional boundary conditions can be obtained [6].

2.1 Renormalization of the vector current

The renormalization condition for the vector current is derived from the vector Ward identity [7],

$$\int_{\partial R} d\sigma_\mu(x) \langle V_\mu^a(x) \mathcal{O}_{\text{int}}^b(y) \mathcal{O}_{\text{ext}}^c(z) \rangle = - \langle [\delta_V^a \mathcal{O}_{\text{int}}^b(y)] \mathcal{O}_{\text{ext}}^c(z) \rangle. \quad (6)$$

By choosing the spacetime region R to consist of all times smaller than x_0 , the only contribution stems from the timeslice x_0 which results in

$$\int d^3\mathbf{x} \langle V_0^a(x_0, \mathbf{x}) \mathcal{O}_{\text{int}}^b(y) \mathcal{O}_{\text{ext}}^c(z) \rangle = - \langle [\delta_V^a \mathcal{O}_{\text{int}}^b(y)] \mathcal{O}_{\text{ext}}^c(z) \rangle. \quad (7)$$

We identify the operators O_{int} and O_{ext} with the boundary fields at $x_0 = 0$ and $x_0 = T$,

$$O^a = a^6 \sum_{\mathbf{u}, \mathbf{v}} \bar{\zeta}(\mathbf{u}) \gamma_5 \frac{\tau^a}{2} \zeta(\mathbf{v}) \quad \text{and} \quad O'^a = a^6 \sum_{\mathbf{u}', \mathbf{v}'} \bar{\zeta}'(\mathbf{u}') \gamma_5 \frac{\tau^a}{2} \zeta'(\mathbf{v}'), \quad (8)$$

where ζ and $\bar{\zeta}$ are the Schrödinger functional boundary fields at $x_0 = 0$ and their primed versions the fields at $x_0 = T$, respectively. After replacing both sides by their renormalized lattice counterparts, we arrive at

$$Z_V(1 + b_V am_q) f_V(x_0) = f_1 + O(a^2), \quad (9)$$

with

$$f_V(x_0) = \frac{a^3}{2(N_f^2 - 1)L^6} \sum_{\mathbf{x}} i \epsilon^{abc} \langle O'^c V_0^a(x_0, \mathbf{x}) O^b \rangle \quad \text{and} \quad f_1 = -\frac{1}{(N_f^2 - 1)L^6} \langle O'^c O^c \rangle. \quad (10)$$

The Ward identity is valid for all x_0 , although boundary effects are expected far from the temporal center of the lattice. In order to get a better handle on statistical fluctuations, we have evaluated the renormalization condition at the central four timeslices and taken the average.

2.2 Improvement of the vector current

The improvement condition for the vector current was first presented in [8] and is based on the axial Ward identity. By insertion of an axial current as an operator inside the spacetime region R we get

$$\int_{\partial R} d\sigma_\mu(x) \langle A_\mu^a(x) A_\nu^b(y) O_{\text{ext}}^c(z) \rangle - 2m \int_R d^4x \langle P^a(x) A_\nu^b(y) O_{\text{ext}}^c(z) \rangle = i f^{abcd} \langle V_\nu^d(y) O_{\text{ext}}^c(z) \rangle. \quad (11)$$

By specifying R as the region between the timeslices $x_0 = t_1$ and $x_0 = t_2$ with $t_1 < y_0 < t_2$, two surface terms arise:

$$\begin{aligned} & \int d^3x \langle [A_0^a(t_2) - A_0^a(t_1)] A_\nu^b(y) O_{\text{ext}}^c(z) \rangle - 2m \int d^3\mathbf{x} \int_{t_1}^{t_2} dx_0 \langle P^a(x) A_\nu^b(y) O_{\text{ext}}^c(z) \rangle \\ & = i f^{abcd} \langle V_\nu^d(y) O_{\text{ext}}^c(z) \rangle. \end{aligned} \quad (12)$$

Since the Ward identity is valid for all ν , we take $\nu = k$. The source operator O_{ext}^c is chosen as

$$O_k^c = a^6 \sum_{\mathbf{u}, \mathbf{v}} \bar{\zeta}(\mathbf{u}) \gamma_k \frac{\tau^c}{2} \zeta(\mathbf{v}), \quad (13)$$

where ζ and $\bar{\zeta}$ are quark fields at the boundary $x_0 = 0$. After implementing this improvement condition in terms of Schrödinger functional correlation functions, one finds

$$Z_A^2 [k_{A_0 A_k}^I(t_2, y_0) - k_{A_0 A_k}^I(t_1, y_0)] - 2m Z_A^2 \tilde{k}_{P A_k}(t_1, t_2, y_0) = Z_V [k_V(y_0) + a c_V \tilde{\delta}_0 k_T(y_0)] + O(a^2), \quad (14)$$

omitting the sea and valence quark mass b -coefficients for brevity; it is to be understood as our final expression, which can be solved for c_V (once Z_V and Z_A are known). For explicit definitions of the correlators we refer, e.g., to [7–10], with contributions that are diagrammatically represented via quark diagrams corresponding to possible Wick contractions in figure 1; more details will be given elsewhere [11]. For the present analysis, (14) was evaluated at $t_1 = T/4$ and $t_2 = 3T/4$, as originally suggested in [8]. Considered as a function of the timeslice variable y_0 , a plateau at the temporal center of the lattice is identified for the (local) $c_V(y_0)$. In order to tame statistical fluctuations, the quoted preliminary values for c_V are extracted as averages of the central two timeslices.

2.3 Ratio of renormalization constants Z_S/Z_P

To derive a renormalization condition for the ratio of quark mass renormalization factors Z_S and Z_P , we exploit a renormalization condition that once more is derived from the massive axial Ward identity — closely following the ALPHA Collaboration’s method to compute Z_A for $N_f = 2, 3$ [9, 10] —, but now relying on a pseudoscalar insertion as internal operator with a behaviour under variation:

$$\delta_A^a P^b(x) = d^{abc} S^c(x) + \frac{\delta^{ab}}{N_f} \bar{\psi}(x)\psi(x). \quad (15)$$

For d^{abc} not to vanish (and thus to ensure sensitivity to the scalar density on the r.h.s. of this equation), one has to work with a $SU(N_f)$ algebra in the valence sector, where $N_f \geq 3$. Here, we choose $SU(3)$, assume $a \neq b$ and adopt a product of two pseudoscalar boundary sources, compare (8),

$$\mathcal{O}_{\text{ext}}^{ba} = \frac{1}{(N_f^2 - 1)L^6} \mathcal{O}^{rb} \mathcal{O}^a \quad (16)$$

as external operator in the integrated axial Ward identity

$$\int_{\partial R} d\sigma_\mu(x) \langle A_\mu^a(x) P^b(y) \mathcal{O}_{\text{ext}}(z) \rangle - 2m \int_R d^4x \langle P^a(x) P^b(y) \mathcal{O}_{\text{ext}}(z) \rangle = -d^{abc} \langle S^c(y) \mathcal{O}_{\text{ext}}(z) \rangle, \quad (17)$$

which is similar to (11) but involves a pseudoscalar density insertion with a variation according to (15). Upon identifying each piece with a Schrödinger functional correlator, some steps of algebra [12] yield a formula that can be solved for Z_P/Z_S (once Z_A is known) and in which the intrinsic scale dependence of the individual renormalization factors drops out, viz.

$$Z_A Z_P [(f_{AP}^{ba})^1(t_2, y_0) - (f_{AP}^{ba})^1(t_1, y_0) - 2m \tilde{f}_{PP}^{ba}(t_2, t_1, y_0)] = -Z_S f_S^{ba}(y_0) + \mathcal{O}(a^2). \quad (18)$$

Again, any b -coefficients are suppressed here. The correlators are defined analogously to those in [7–10], and their explicit forms will be given fully elsewhere [12]. Quark diagrams with possible Wick contractions for the $f_{\Gamma\tilde{\Gamma}}(x_0, y_0)$ contributing to the l.h.s. of this equation are illustrated in figure 1.

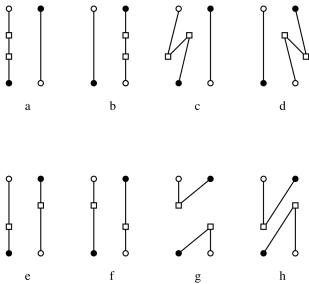


Figure 1. Graphical representation (figure borrowed from [7]) of possible Wick contractions for correlation functions of generic form $f_{\Gamma\tilde{\Gamma}}(x_0, y_0)$ with quark bilinear insertions Γ and $\tilde{\Gamma}$, appearing on the l.h.s. of (18). Filled (open) circles stand for the creation (annihilation) of a quark at the boundaries of the lattice, while squares indicate insertions of local composite fields. In a first trial analysis, we had evaluated (18) for insertion points $y_0 = T/2$, $t_1 = T/3$ and $t_2 = 2T/3$. Still, we do not quote any results for Z_P/Z_S in this status report, because a careful study to extract it from the renormalization condition proposed here has only started after the conference.

3 Simulation details

As improvement coefficients and renormalization factors are short-distance quantities, they can be extracted by imposing suitable conditions in a finite (i.e., in practice, small) physical volume. This is realized by the Schrödinger functional framework, governed by periodic boundary conditions in space and Dirichlet ones in time. The gauge field configuration ensembles used in this work are almost identical to the ones that were generated in the context of the improvement and renormalization of the

$L^3 \times T/a^4$	β	κ	#REP	#MDU	ID
$12^3 \times 17$	3.3	0.13652	20	10240	A1k1
		0.13660	10	13672	A1k2
		0.13648	5	6876	A1k3
$14^3 \times 21$	3.414	0.13690	32	10176	E1k1
		0.13695	48	13976	E1k2
$16^3 \times 23$	3.512	0.13700	2	20480	B1k1
		0.13703	1	8192	B1k2
		0.13710	3	22528	B1k3
$16^3 \times 23$	3.47	0.13700	3	29560	B2k1
$20^3 \times 29$	3.676	0.13700	4	15232	C1k2
		0.13719	4	15472	C1k3
$24^3 \times 35$	3.810	0.13712	6	10272	D1k1
		0.13701	3	5672	D1k2
		0.13704	1	800	D1k3

Table 1. Summary of simulation parameters of the gauge configuration ensembles used in this study, as well as the number of (statistically independent) replica per ensemble ‘ID’ and their total number of molecular dynamics units. Bold ID’s indicate three new ensembles compared to [4, 10].

axial vector current [4, 10] and cover the β -range of the $N_f = 3$ large-volume QCD configurations of the CLS effort, corresponding to lattice spacings of about ($0.05 \lesssim a \lesssim 0.09$) fm [13, 14]. Their specifications are collected in table 1. To supplement the data base of configurations already available from [4, 10], the production of a few new ensembles — labeled by A1k3, D1k2 and D1k3 in the table — was started. These ensembles exhibit a more chiral (i.e., closer to zero) mass of the three mass-degenerate sea quarks and thereby allow for getting a better handle on the mass dependencies of the quantities of interest that will prove to be essential in the case of c_V .

Compared to the previous $N_f = 0$ study [8], we have implemented various refinements: First of all, as detailed in [4], all gauge field ensembles entering the analysis lie on a line of constant physics characterized by a fixed spatial physical volume of $L \approx 1.2\text{fm} = \text{constant}$, $T \approx 3L/2$ and almost vanishing mass of the (degenerate) sea quarks. The valence quark mass in the computation of correlation functions equals the sea quark value. This entails that the renormalization and improvement factors become smooth functions of the bare coupling, i.e., $g_0^2 = 6/\beta$. Only the ensemble B2k1 deliberately misses the condition of fixed physical volume and is used to quantitatively investigate the effect of such a deviation on the results. Furthermore, again following [4], the Schrödinger functional correlation functions incorporate optimized boundary wave-functions, in order to suppress excited state effects and thus to maximize the overlap with the ground state in their spectral decomposition. Finally, for the case of c_V , we also have identified the importance of the additional mass term in the axial Ward identity, (14), the impact of which will be discussed in the results section. In this context, we have tested different sets of insertion times for the individual operators and found a specific choice that seems to reduce the effects caused by the non-zero mass comprehensively.

The statistical error analysis of the Markov chain Monte Carlo data utilizes the Γ -method based on evaluating autocorrelation functions [15] and was cross-checked against binned Jackknife estimates.

4 Results

The analysis underlying the results presented here was done including all topological sectors. By virtue of the theoretical argument that our results — being based on Ward identities, as operator identities holding in any topological sector — should be insensitive to the topological charge Q_{top} , we

believe that the influence of restricting the computations to one sector of fixed Q_{top} (say, $Q_{\text{top}} = 0$) is negligible, modulo the accompanying reduction of statistics. This expectation still needs to be confirmed in the final analysis, though.

The left panel of figure 2 shows an representative evaluation of the local PCAC quark mass, $am_{\text{PCAC}}(x_0)$, on the gauge configurations of ensemble C1k3. The actual values for all PCAC masses entering our analysis are always chosen as plateau averages over the central $L/2$ timeslices of the temporal extent of the lattice. Thereby it is guaranteed that also these averaging intervals are scaled in physical units in the same way as all other length scales, in order to obey the constant physics condition in all steps of the computation.

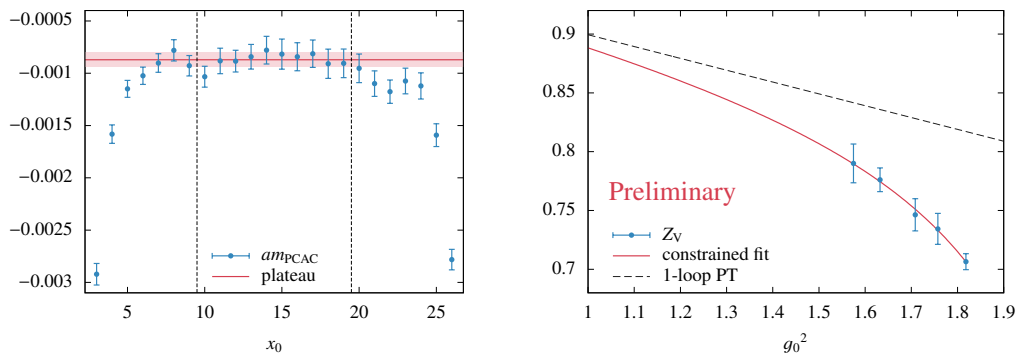


Figure 2: *Left:* Exemplary results for am_{PCAC} on different timeslices, evaluated on the C1k3 ensemble. The dashed vertical lines span the plateau region of the central $L/2$ timeslices, over which the plateau average is taken. *Right:* Results for Z_V together with an interpolating fit, constrained by 1-loop perturbation theory [16].

4.1 Z_V

Results for the vector renormalization constant Z_V are presented in the right panel of figure 2, in comparison to 1-loop perturbation theory taken from [16]. The individual data points, obtained by a chiral extrapolation to zero (valence = sea) quark mass using b_V in (9) from [1, 2] (but neglecting the corresponding b -coefficient in the sea quark sector), show a smooth behavior that is well described by a polynomial fit constrained by perturbation theory. The preliminary interpolation formula reads:

$$Z_V(g_0^2) = 1 - 0.10057g_0^2 \times \frac{1 - 0.388(13)g_0^2}{1 - 0.449(8)g_0^2}. \quad (19)$$

4.2 c_V

As outlined above, the condition of [8] to fix the vector current improvement coefficient c_V is extended by accounting for an additional term that naturally arises when the Ward identity is employed at finite quark mass, cf. (14). The impact of this term is demonstrated in the left panel of figure 3, where the chiral extrapolations (using values for the associated valence quark mass b -coefficients from [1, 2]) for $L/a = 16$ and $g_0^2 = 1.7084$ ($\beta = 3.512$) with and without the mass term are compared with each other. Although both extrapolations nicely meet in almost the same chiral limit at $am_{\text{PCAC}} = 0$, the data without inclusion of the mass term show a much steeper behaviour. This finally results in a larger error at $am_{\text{PCAC}} = 0$ and thus underlines the importance of refining the improvement condition for c_V through accounting for the mass term in the analysis even at small but finite quark masses.

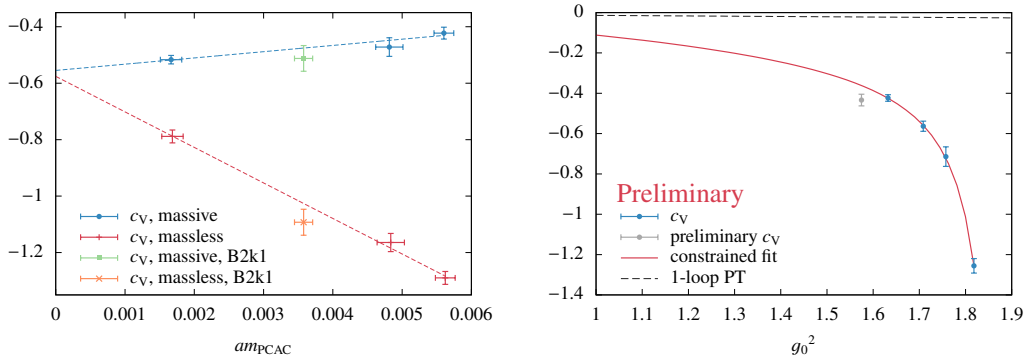


Figure 3: *Left:* Chiral extrapolation of c_V at $L/a = 16$ and $g_0^2 = 1.7084$ ($\beta = 3.512$) for the case with and without including the additional mass term in the Ward identity. The data points from the ensemble B2k1 indicate that a sizeable violation of the constant physics condition does not influence our results appreciably. *Right:* Results for c_V together with an interpolating fit, constrained by 1-loop perturbation theory [17]. The gray data point refers to a tentative analysis on the gauge configuration ensembles D1k2 and D1k3, whose generation was launched during the conference. Hence, it is only indicative and not yet included in the fit.

Additionally, to quantitatively check for the influence of a violation of the constant physics condition on our analysis, results from the gauge configuration ensemble B2k1 are displayed in the same figure. This ensemble (see table 1) has a β -value shifted by an amount, which corresponds to a $\sim 6\%$ shift in the spatial extent of the physical volume, and thus induces a significant deviation from our condition $L \approx 1.2\text{fm} = \text{constant}$. As can be seen in the left panel of figure 3, these data points align fairly well with the other points along the (linear) fit function. Hence, we conclude that any deviations from the constant physics condition of this order of magnitude or below are of only minor influence and can safely be neglected on the level of the final precision for c_V .¹ Note that this is also in line with the findings already reported in [4, 10].

The preliminary estimates for c_V are presented in the right panel of figure 3, together with the prediction from 1-loop perturbation theory that we have extracted for our lattice action from the perturbative results in [17]. The gray data point stems from the ensembles D1k2 and D1k3 (see table 1). Since the generation of these gauge field configurations was only started during the conference and is still ongoing, we exclude it from the subsequent analysis steps for the purpose of the present status report. Nevertheless it is reassuring that this — so far only indicative — result appears to blend in well with the g_0^2 -dependence of the other points.

At this point, we therefore describe our results for c_V by a preliminary interpolating Padé fit, constrained by 1-loop perturbation theory in the asymptotic $g_0^2 \rightarrow 0$ regime, as

$$c_V(g_0^2) = -0.01030(4)g_0^2 C_F \times \frac{1 + 5.80(47)g_0^2 - 2.99(30)g_0^4}{1 - 0.532(1)g_0^2}, \quad C_F = \frac{4}{3}, \quad (20)$$

where, as stressed above, the gray point in the right plot of figure 3 is not included in the fit. Moreover, any uncertainties originating from Z_V or Z_A (entering the final formula for c_V according to (14)) have not yet been propagated into the errors on c_V quoted in the figure such that we still expect them to slightly increase after a final analysis. Note that, in qualitative agreement with observations already made in the exploratory quenched study [8], the non-perturbative c_V substantially deviates

¹The same holds true for our results on Z_V .

from perturbation theory in the range of bare couplings (resp. β -values) typically encountered in large-volume applications with the lattice action employed here.

5 Outlook

For the completion of our work to determine the renormalization and improvement factors discussed in this report it essentially remains to 1.) evaluate the relevant correlators for the full statistics on all ensembles of table 1, 2.) check for independence of the results on topology by repeating the computations in the sectors of fixed Q_{top} , 3.) quantify the size of possible $O(a)$ ambiguities in improvement (resp. renormalization) conditions for the vector current and, in particular, 4.) to also perform the data analysis to extract the ratio Z_S/Z_P . For a related study to calculate improvement b -coefficients in the valence sector, multiplying mass dependent $O(a)$ Symanzik counterterms to local operators, as well as the ratio $Z_m Z_P/Z_A$ of quark mass renormalization constants, see [18].

Acknowledgements

We thank P. Fritzsch, S. Sint, R. Sommer, S. Kuberski and G. Bali for helpful discussions. This work was supported by grant HE 4517/3-1 (J. H. and C. W.) of the *Deutsche Forschungsgemeinschaft*. We gratefully acknowledge the computer resources provided by the *Zentrum für Informationsverarbeitung* of the University of Münster (PALMA HPC cluster) and thank its staff for support.

References

- [1] P. Korcyl, G.S. Bali, Phys. Rev. **D95**, 014505 (2017), 1607.07090
- [2] P. Korcyl, G.S. Bali, PoS **LATTICE2016**, 190 (2016), 1609.09477
- [3] J. Bulava, S. Schaefer, Nucl. Phys. **B874**, 188 (2013), 1304.7093
- [4] J. Bulava, M. Della Morte, J. Heitger, C. Wittemeier, Nucl. Phys. **B896**, 555 (2015), 1502.04999
- [5] M. Dalla Brida, S. Sint, P. Vilaseca, JHEP **08**, 102 (2016), 1603.00046
- [6] M. Dalla Brida, S. Sint, PoS **LATTICE2014**, 280 (2014), 1412.8022
- [7] M. Lüscher, S. Sint, R. Sommer, H. Wittig, Nucl. Phys. **B491**, 344 (1997), hep-lat/9611015
- [8] M. Guagnelli, R. Sommer, Nucl. Phys. Proc. Suppl. **63**, 886 (1998), hep-lat/9709088
- [9] M. Della Morte, R. Hoffmann, F. Knechtli, R. Sommer, U. Wolff, JHEP **07**, 007 (2005), hep-lat/0505026
- [10] J. Bulava, M. Della Morte, J. Heitger, C. Wittemeier, Phys. Rev. **D93**, 114513 (2016), 1604.05827
- [11] J. Heitger, F. Joswig, to be published
- [12] J. Heitger, F. Joswig, A. Vladikas, to be published
- [13] M. Bruno et al., JHEP **02**, 043 (2015), 1411.3982
- [14] M. Bruno, T. Korzec, S. Schaefer, Phys. Rev. **D95**, 074504 (2017), 1608.08900
- [15] U. Wolff, Comput. Phys. Commun. **156**, 143 (2004), [Erratum: Comput. Phys. Commun. **176**, 383 (2007)], hep-lat/0306017
- [16] S. Aoki, K. Nagai, Y. Taniguchi, A. Ukawa, Phys. Rev. **D58**, 074505 (1998), hep-lat/9802034
- [17] Y. Taniguchi, A. Ukawa, Phys. Rev. **D58**, 114503 (1998), hep-lat/9806015
- [18] G.M. de Divitiis, M. Firrotta, J. Heitger, C.C. Köster, A. Vladikas, *Non-perturbative determination of improvement b-coefficients in $N_f = 3$* , in *35th International Symposium on Lattice Field Theory (LATTICE 2017), Granada, Spain*, to appear in EPJ Web of Conf. (2017), 1710.07020